2020 IEEE International Conference on Robotics and Automation (ICRA)
31 May - 31 August, 2020. Paris, France

Automated Tracking System with Head and Tail Recognition for Time-Lapse Observation of Free-Moving C. elegans

Shengnan Dong, Xiaoming Liu, *Member, IEEE*, Pengyun Li, Xiaoqing Tang, Dan Liu, Masaru Kojima, Qiang Huang, *Fellow, IEEE*, Tatsuo Arai, *Fellow, IEEE*

***Abstract*—In this paper, an automated tracking system with head and tail recognition for time-lapse observation of free-moving C. elegans is presented. In microscale field, active C. elegans can move out of the view easily without an automated tracking system because of the narrow field of view and rapid speed of C. elegans. In our previous works, we constructed an automated platform with 3D freedom to track centroid region of the nematode successfully. However, tracking time was not long enough to support a full time-lapse observation. Our proposed system in this study integrate the detection method in horizontal plane with depth evaluation more tightly. Tracking time and response speed have been greatly improved. Besides, we make full use of curvature calculation to make the system recognize the head and tail of C. elegans and the recognition rate can be up to 95%. The results demonstrate that the system can fully achieve automated long-term tracking of a free-living nematode and will be a nice tool for C. elegans behavioral analysis.**

I. INTRODUCTION

The nematode Caenorhabditis elegans (C. elegans) is widely used in the areas of neuroscience, medicine development and genetic control mechanism [1-3]. C. elegans is a small worm with a length of about 1 mm. It has a fast life cycle of approximately 3 days and a short lifespan of only 2 weeks [4-5]. Besides, it is one of the simplest organisms with a nervous system comprising only 302 neurons [6-7]. Moreover, because of fully completely sequenced genome and thorough development patterns, C. elegans becomes one of the most useful model organisms. It plays a crucial role in study of molecular mechanisms of apoptosis [8-9] and the small RNAs gene silencing [10]. Thus, there is a great demand for automatic observation and manipulation of C. elegans. A variety of microscopic systems for observation and analysis of C. elegans behavior have been described. However, most of them are constructed in microfluidic devices [11-14] which includes many separate chambers on a chip. Although they can achieve long-term observation, the living space of the nematodes is highly restricted. Even worse, the nematode is limited to a certain place when C. elegans is fixed by the narrow channel. It is difficult to study real behavior of C. elegans in nature environment through those systems. Therefore, we are proposed to make an automatic tracking system for free-moving C. elegans. Because C. elegans is a typical example that the object can rapidly move out of the microscope field without an automatic tracking system during monitoring [15-19]. There are two main challenges as follows: 1) due to the extremely narrow microscope field and the agile movement of C. elegans, objects disappear from the field of view frequently; 2) captured images are often defocused by the small microscopic depth.

In the previous work, we have developed an automatic tracking system that can keep C. elegans always at the center of the field of view [20]. However, our tracking time at that time was not long enough to ensure a long-time observation without any manual works. Current improved system can track C. elegans more than 2 hours and find focal plane more rapidly. In a variety of studies, we need to experiment with particular regions like head region sometimes. Therefore, the desire to recognize the head and tail efficiently arises. In the meanwhile, head recognition can also help the system to predict the movement of the nematode and improve tracking. It is popular to use template matching to track particular region of C. elegans [21] which is lack of applicability to dynamically changing regions. Also, fluorescent protein is used to help track particular region. We consider to use the curvature for head and tail recognition, which is more applicable and harmless. Because the bending of the head and tail is very different during movement. Curvature can represent the bending degree of C. elegans and has been applied to many methods like corner detector [22], curve-fitting [23] and so on. The curvature has ability to reflect bending degree and help distinguish the head and tail. However, we need face the challenge to apply the curvature to discrete points in digital pictures.

The paper is organized as follows: in Section II, we introduce details about curvature evaluation of captured images. In Section III, we introduce methods about detection in X-Y plane and depth evaluation in Z-axis. Section IV describes experimental preparation and shows the experimental results.

This work was supported by the National Natural Science Foundation of China under Grants (61873037, 61903039), China Postdoctoral Science Foundation (BX20190035) and the Grant-in-Aid for Scientific Research (19H02093) from the Ministry of Education, Culture, Sports, Science and Technology of Japan.

S. Dong, X. Liu, P. Li, X. Tang, D. Liu, M. Kojima, Q. Huang and T. Arai are with Intelligent Robotics Institute, School of Mechatronical Engineering, Beijing Institute of Technology, Beijing, China and Beijing Advanced Innovation Center for Intelligent Robots and Systems (Beijing Institute of Technology), Beijing, China *(Corresponding author: X. Liu, e-mail: liuxiaoming555@ bit.edu.cn)*.

Masaru Kojima is with the Department of Materials Engineering Science, Osaka University, 1-3, Machikaneyama, Toyonaka, Osaka, 560-8531, Japan Osaka University. Tatsuo Arai is also with the Global Alliance Lab., the University of Electro-Communications, Tokyo, Japan.

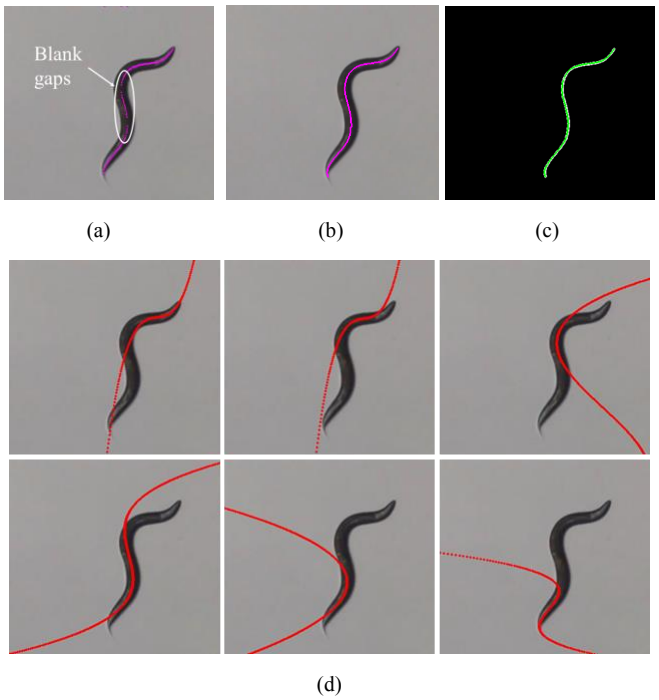

Figure 1. Fitting results. (a) fitting directly. (b) fitting with pre-processing. (c) the fitting curve with the skeletonized curve (the white one represents the skeletonized curve and the green one represents the fitting curve). (d) fitting of each segment

II. CURVATURE EVALUATION

A. Curvature calculation

For a plane curve, curvature can mathematically indicate the degree of bending at a certain point. The center of curvature is defined as the intersection point of two infinitely close normals of the curve. And the radius of curvature is the distance from the center of curvature to the curve. As for the curvature, it is the reciprocal of the radius of the curvature. The magnitude of the curvature is positively related to the degree of bending of the curve. The greater the curvature of the plane curve, the more severe bending the curve has.

When the curve is continuous, curvature has a strict mathematical definition. For the case of a plane curve given explicitly as the graph of a function y = f(x), we can process curvilinear function easily to obtain the curvature k through the equation as shown in the following:

$$k = \frac{y''}{(1+y'^2)^{\frac{3}{2}}} \tag{1}$$

The equation cannot be applied to the images captured by the system. We can skeletonize the nematode detected to get corresponding representative curve whose width is only 1 pixel. However, in the field of visual and image analysis, what we can get from the camera is digital images or digital curves. Hence, the curve processed from the original captured picture is actually a set of discrete points.

B. Curvature processing

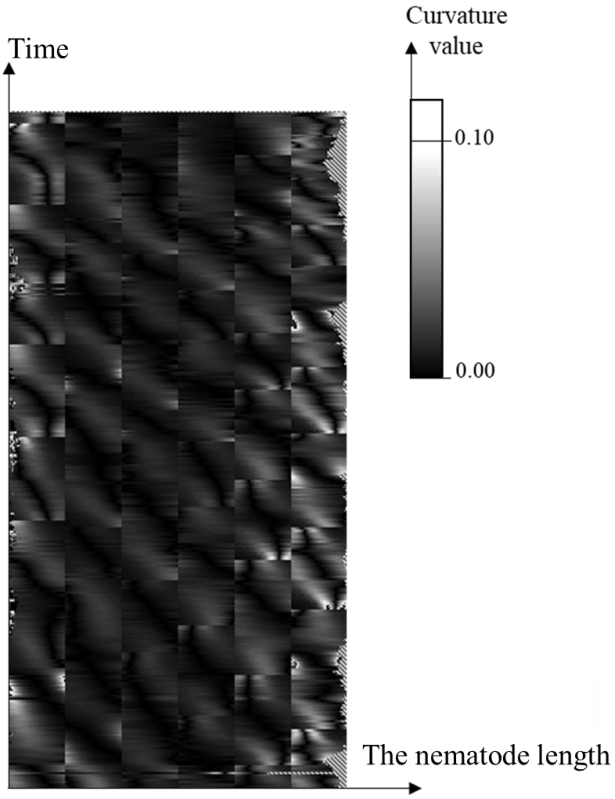

Figure 2. A temporal curvature map of an example of curvature changes at every point of the nematode over a period of time. There is a linear relationship between grey level of each pixel and curvature value: when the curvature value is greater than or equal to 0.1, the grey level is 255 which means white; in the meanwhile, if the curvature value is 0, the grey level is 0 which means black.

There are numerous calculation methods for the curvature in discrete cases, the most intuitive of which is difference operator. For the difference operator, it can directly covert the calculation formula into the equation about the neighbor points. But it turns out the small noise on the curve will have a catastrophic effect on the curvature calculation. Besides, it only considers the information near a particular point rather than the overall situation of this part of curve. In our case, the curvature value calculated by the difference operator often shows zero value which is seriously inconsistent with the reality. In order to solve these problems, many researchers have proposed a variety of calculating methods for the discrete curvature, such as k-cosine curvature calculation method [24], k-corner curvature calculation method [25] and so on. When applying these mainstream discrete curvature methods to our captured pictures, the changing trend of curvature was very abnormal that obviously not in line with the degree of curvature observed by the naked eye. Thus, we choose to fit the discrete points into a function of continuous curve firstly to get curvatures. Before fitting, we need to sort these points in order so that we can fit properly from one end of the curve to the other end.

The method of least squares is a mathematical optimization method that can find the best function match for the data by minimizing the sum of the squares of the errors. In our system, we select the polynomial in a single indeterminate x as the target function as shown in the following:

$$y = a_n x^n + a_{n-1} x^{n-1} + \cdots + a_2 x^2 + a_1 x + a_0 \quad (2)$$

It is almost impossible to fit all discrete points in the same curve function. We should split the point set into m parts and fit them separately. After a series of experiments and comparisons, we find that when the value of m is 6 and the value of n is 3, the result seems to be the best. However, the curve obtained by the fitting still exists the problem that there are some blank gaps (shown in Fig. 1(a)), which will affect curvature calculation strongly. As marked in the figure, the blank gaps appear frequently in the fitting curve. This is because the same x value corresponds to multiple y values in the segment of the curve which violates the definition of the function. It leads to a serious deviation in the curve fitting which brings blank gaps. Therefore, we will pre-process each part of the point set: 1) count the number of points whose x value corresponds to multiple y values; 2) calculate its proportion in the segment; 3) if the proportion exceeds a certain threshold, make a homogeneous coordinate transformation that exchange the x value and y value. After such pretreatment, curve fitting shows a good result in the fitting of each segment as shown in Fig. 1(d). In every segment, the method fits the discrete points to a continuous curve which can represent the part of nematode body well. When combining the fitting curve of each segment, we can get the continuous piecewise curve function without any blank gaps like Fig. 1(b). Comparing the fitting result with skeletonized curve, the fitting error is small enough to ignore (shown in Fig. 1(c)). Finally, the system can use the piecewise function to calculate the curvature of every point in the fitting curve. In order to more clearly illustrate the curvature changes at every point of the nematode over a period of time, we generate a temporal curvature map as shown in Fig. 2. We set up such a linear relationship between grey level of each pixel and curvature value: when the curvature value is greater than or equal to 0.1, the grey level is 255 which means white; in the meanwhile, if the curvature value is 0, the grey level is 0 which means black. For the curvature map, the horizontal axis changes along the nematode length, and the vertical axis changes with time. The curvature map shows the curvature of each point along the nematode body as time goes by. Obviously, the white part which means high curvature moves along the nematode body.

III. PROCESSING METHOD

A. C. elegans detection

Under the microscope, the field of view is too narrow for the movement of C. elegans, which causes that nematodes to move out of the view easily without an automated tracking system. It is necessary to use a fast and accurate detection method in horizontal plane to update the position of the target in real-time. Also, the background in the microscopic environment is relatively simple and clean. Therefore, the traditional method contour detection can basically meet the detection requirement of the nematode. However, the movement of C. elegans with long-time experiment can leave traces which will affect contour detection. Thus, we take a deep learning model to our detection method to make the system perform better. Because our system requires real-time processing and high accurate ratio, we apply YOLO (You Only Look Once: United, Real-Time Object Detection, 2016) model to improve detection method. The fast version YOLO model runs at more than 150 frames per second in a good configuration [26]. It is accurate enough to detect C. elegans because the background in micro scale is simpler and more monotonous. Aiming to achieve a more precise positioning, we use the YOLO model firstly to search regions just include C. elegans. Then the system can make full use of contour detection to draw the outlines of nematodes within the range detected previously. Besides, the system takes the area as one of the judgement factors to filter wrong detections. Eventually, we can calculate the real-time position of the target point like

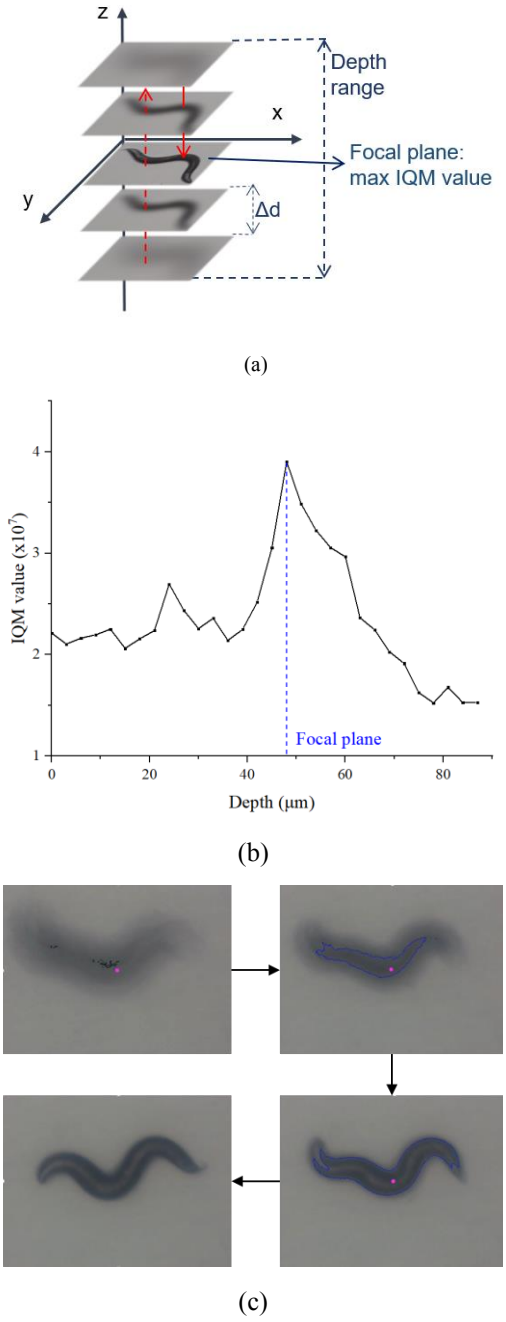

Figure 3. Autofocusing results on C. elegans. (a) Process of autofocusing based on IQM value; (b) Relative curve between IQM value and the depth information; (c) Autofocusing process on C. elegans.

the centroid from the detected contour information.

B. Depth evaluation

In order to track C. elegans all the time, we need to solve the problem caused by depth of field restriction and make it always in focus. In the microscopic environment, current autofocus methods typically require a process of defocusing, focusing, and defocusing repeatedly. The essential of autofocus is the evaluation of fixing the image to focus. There are many ways to analyze each image captured using different evaluation functions, such as image gray-scale variance functions.

In our system, the evaluation function is applied to all pixels of a particular captured image as follows:

$$IQM(j)=\frac{1}{D}\sum_{x=x_i}^{x_f}\sum_{y=y_i}^{y_f}\left\{\sum_{p=-L_e}^{L_e}\sum_{q=-L_r}^{L_r}|I(x,y)-I(x+p,y+P)|\right\} \quad (3)$$

$(1 < j < N)$

Where IQM (Image Quality Measurement) is an evaluation value that reflects the level of focus. When the IQM value is larger, the number of pixels in the focus becomes larger. We can get this value by applying a Laplacian filter and then using a smoothing filter for each pixel of the captured image. In the equation, $(-L_e, -L_r) - (L_e, L_r)$ and $(x_i, y_i) - (x_f, y_f)$ represents the ROI (region of interests) using the Laplacian filter and the smoothing filter. As for D, it represents the total number of pixels in the ROI [27]. N represents the number of images we apply to the evaluation function.

As shown in Fig. 3(a), the system begins to calculate the IQM value of the image only when an object is detected by YOLO model. Because the plane is clearly far from the focal plane during the period when the system is difficult to detect the target. In the ideal case, the local maximum does not appear in the IQM values. Once the data is in a downward trend, the system can determine the depth of focal plane. However, local maxima often occur in real cases. To eliminate this problem, the system does not stop the calculation until the system cannot detect any objects multiple times. The system then returns the depth at which the IQM value is greatest during the calculation. By using this method, we achieved autofocus during the experiment. Taking microbeads as an example, the relative curve in Fig. 3(b) shows the relationship between the calculated IQM value and depth information, which can be applied to depth measurements under an inverted microscope. In addition, the autofocus process on the nematode typically takes 2 seconds for the first time when the system detects an object (Fig. 3(c)). For subsequent autofocusing procedures, the mean required time reduced to less than 1s which can meet tracking in z-axis. Besides, the success rate is nearly 95% if the system can detect the target.

C. Head and tail recognition

Similar to the snake, C. elegans crawls in a “S” shape. Intuitively, the head and tail of the nematode show different degree of bending when moving forward. We believe that the head bends more than the tail in the movement in most cases. As mentioned previously, we can calculate the curvature value of each point of the nematode with a high accuracy. In the head and tail recognition, we only need consider the curvature at both end regions of the curve. Therefore, we calculate the curvature value of each point in the region at both ends of the skeletonized curve. Then we add these curvature values in two regions separately to get two reference values. If the value is bigger, we will identify the region is head region. However, wrong recognitions appear frequently.

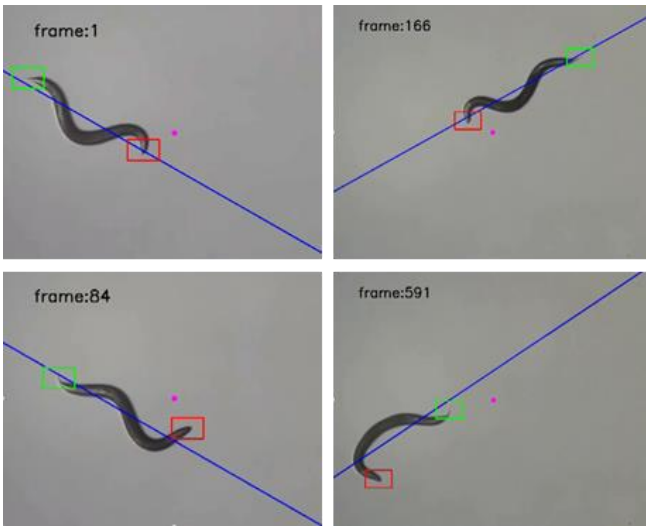

Figure 4. Example of head and tail recognition. Red box: head region. Green box: tail region. Blue line: a straight line obtained by fitting C. elegans

We found that the head region looks straight occasionally during the process of large bending. In these cases, the recognition only based on curvature does not work. Another reference factor should be considered to help recognize head and tail. Firstly, the nematode is fitted into a blue straight line as shown in Fig. 4. After comparison and observation, the head is always farther from the blue line than the tail when the head region looks like a straight line. Therefore, in addition to the sum of curvature values, we also compare the farthest distance from the fitted blue line in the both end region of the curve. With these two reference features, the system can recognize the head and tail of C. elegans successfully.

IV. Experimental Results and Discussion

A. Experimental preparation

Nematode culture and construction of the system were the main contents of experimental preparation. We used wild type Caenorhabditis elegans (C. elegans) Bristol strain N2 as our experimental object to check the tracking performance of the system. All the tacking experiments were carried out in petri dishes containing solid NGM (Nematode Growth Medium). The digital camera had a frame rate of 120 [fps] and the size of images was 640 x 480 [pixels].

In this paper, the system is expected to allow for time-lapse tracking of C. elegans. With robust image processing, our automated platform should keep the object in the center of the microscope's field of view and keep the object constantly in the focal plane. The tracking system consists of two subsystems: a visual part and an execution part. The configuration of each subsystem is as follows:

The visual part provided the main image feedback information for tracking and manipulation. It included an inverted microscope (IX73, Olympus, Inc.) placed on a

vibration isolation table (SAHT-1510K5, Meiritz, Inc.), a digital camera connected to the microscope to collect real-time images, and a Windows PC (Optiplex-9020, Dell, Inc.) which processed the image captured by the digital camera and sended the command to the execution section.

In the execution section, we built an automatic stage that combined the movements in three directions. Most of the platform included a fine X-Y-Z micromanipulator (Sigmakoki, TAM-655) with a linear actuator (Sigmakoki, SGSP-13ACT-B0) on each axis. All three actuators were powered by a 5-phase stepper motor driver (Sigmakoki, SG-55MA). In addition, the 3D printing platform was coupled to a micromanipulator to maintain C. elegans. And the m-bed linked to the PC made the vision part and the execution part together.

B. *Tracking results*

Through a series of experiments, we confirmed that our proposed system can track the centroid region of C. elegans and keep the nematode always in focus during time-lapse. We have accomplished automated tracking for about 2 hours. The end of the tracking experiment was not because the target was missing but due to memory limitations from computer equipment at that time. Experiments show that the system can make up for the position error between the target point and the microscopic vision center for a long time. It indicates that the system has the capability to achieve an automated time-lapse observation. Fig. 5(a) shows an example of pictures that the system can keep target point of C. elegans always in the center of the field of vision for a long time. As shown in Fig. 5(b) and Fig. 5(c), the response capability of the system is so fast that the nematode can move to the center quickly. Steady-state errors along the X-axis and Y-axis are basically less than 5 pixels in the tracking.

As for head and tail recognition, we have applied the method to C. elegans several times. As so far, the recognition rate is around 95%. The wrong recognition may come from the lack of reference features. The sum of curvature of value and the farthest distance are likely not to be sufficient to distinguish all situations.

C. *Discussion*

Experiments so far indicate that our system performs well in real-time tracking of nematodes. Also, the system can recognize head and tail of C. elegans with a high success rate. In the future work, the system can fully integrate head and tail recognition and automatic tracking, as well as operating tools such as pipettes to conduct further experimental analysis of nematodes. Besides, our proposed system can be useful for the analysis of the behaviors of C. elegans because free-moving objects are more conducive to study.

V. CONCLUSION

We propose an automated microscopic feedback system which tracks the particular region of free-moving C. elegans for a long time. Typical contour detection is used to search C. elegans in X-Y plane and IQM values is applied to achieve autofocusing. Also, we train out a good YOLO model which helps to accelerate autofocusing and improve the detection in X-Y plane. Besides, the system can recognize the head and

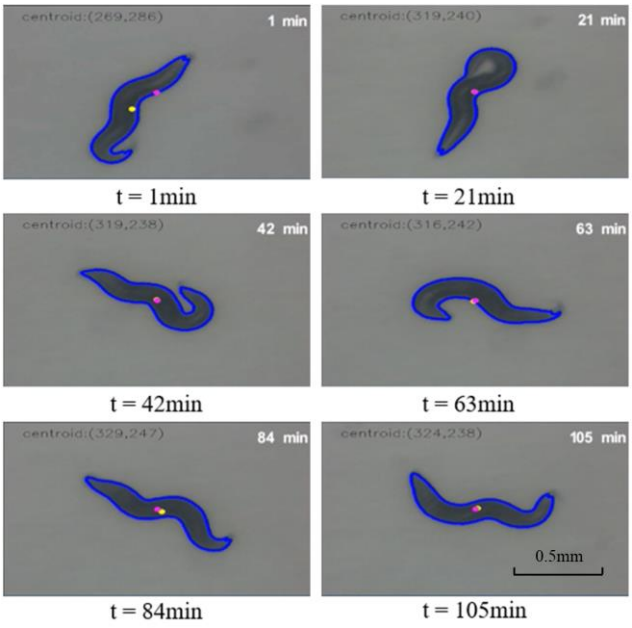

(a)

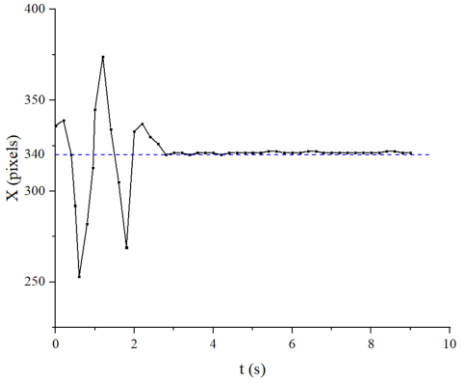

(b)

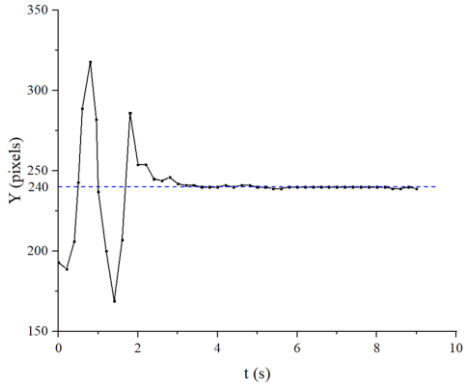

(c)

Figure 5. Experimental results. (a)Examples of images of automated tracking of C. elegans by our proposed system. Pink point: target position. Yellow point: real position. Blue contour represents detected body. The passing time is written in the upper right corner. (b) Relative curve between time and X-axis coordinates of the object. (c) Relative curve between time and Y-axis coordinates of the object.

tail of C. elegans based on curvature calculation. According to the experimental results, we can find that the system can fully achieve automated long-term tracking of a free-living nematode and will be a nice tool for C. elegans behavioral analysis.

Manipulation of the platform is limited in 3D while there is a large need to select a certain pose of C. elegans in many experiments. Our future work is to expand the freedom of the platform, such as increasing a freedom from the rotation on X-Y plane. In Fig. 4, we have already generated a line to represent one of features of posture of C. elegans. We can control the direction of C. elegans with the generated line and a rotary stage. Also, we should make experiments like head tracking with head and tail recognition. Furthermore, we can analyze motion mode of C. elegans with curvature map.

ACKNOWLEDGMENT

This work was supported by the National Natural Science Foundation of China under Grants (61873037, 61903039), China Postdoctoral Science Foundation (BX20190035) and the Grant-in-Aid for Scientific Research (19H02093) from the Ministry of Education, Culture, Sports, Science and Technology of Japan.

REFERENCES

[1] J. Yochem and R. K. Herman, "Investigating C. elegans development through mosaic analysis," *Development*, vol. 130, no. 20, pp. 4761-4768, 2003.

[2] R. Nass, D. H. Hall, D. M. Miller, and R. D. Blakely, "Neurotoxin-induced degeneration of dopamine neurons in Caenorhabditis elegans," *Proc. Natl. Acad. of Sciences of the United States of America*, vol. 99, no. 5, pp. 3264-3269, 2002.

[3] T. A. Scott et al., "Host-Microbe Co-metabolism Dictates Cancer Drug Efficacy in C. elegans," *Cell*, vol. 169, no. 3, pp. 442-456, 2017.

[4] J. E. Sulston and H. R. Horvitz, "Post-embryonic Cell Lineages of the Nematode Caenorhabditis elegans," Developmental Biology, vol. 56, no. 1, pp. 110–156, 1977.

[5] C. J. O'Kane, "Modelling human diseases in Drosophila and Caenorhabditis," *Seminars in Cell & Developmental Biology*, vol. 14, pp. 3-10, 2003.

[6] A. Sakaguchi-Nakashima, J. Y. Meir, Y. Jin, K. Matsumoto, N. Hisamoto, "LRK-1, a C. elegans PARK8-related Kinase, Regulates Axonal-dendritic Polarity of SV Proteins," *Curr. Biol.*, vol. 17, pp. 592-598, 2007.

[7] A. Ghosh-Roy, A. D. Chisholm, "Caenorhabditis elegans: a new model organism for studies of axon regeneration," *Dev. Dyn*., vol. 239, pp. 1460-1464, 2010.

[8] H. M. Ellis and H. R. Horvitz, "Genetic Control of Programmed Cell Death in the Nematode Caenorhabditis Elegans," *Cell Biology International Reports*, vol. 44, no. 6, pp. 817-829, 1986.

[9] J. Yuan and H. R. Horvitz, "The Caenorhabditis elegans genes ced-3 and ced-4 act cell autonomously to cause programmed cell death", *Dev. Biol*, vol. 138, no. 1, pp. 33-41, 1990.

[10] A. Grishok, "Biology and Mechanisms of Short RNAs in Caenorhabditis elegans," *Advances in Genetics*, vol. 83, pp. 1-69, 2013.

[11] S. E. Hulme, S. S. Shevkoplyas, A. P. McGuigan, J. Apfeld, W. Fontana, and G. M. Whitesides, "Lifespan-on-a-chip: Microfluidic chambers for performing lifelong observation of C. elegans," *Lab Chip*, vol. 10, pp. 589-597, 2010.

[12] J. Krajniak and H. Lu, "Long-term high-resolution imaging and culture of C. elegans in chip-gel hybrid microfluidic device for developmental studies," *Lab on a Chip*, vol. 10, pp. 1862-18682010.

[13] W. Keil, L. M. Kutscher, S. Shaham, and E. D. Siggia, "Long-Term High-Resolution Imaging of Developing C. elegans Larvae with Microfluidics," Dev. Cell, vol. 40, no. 2, pp. 202-214, 2017.

[14] N. Chronis, M. Zimmer, and C. I. Bargmann, "Microfluidics for in vivo imaging of neuronal and behavioral activity in Caenorhabditis elegans," *Nat. Methods*, vol. 4, no.9, pp 727-731, 2007.

[15] E. Fontaine, J. Burdick, and A. Barr, "Automated tracking of multiple C. Elegans," in *Annual International Conference of the IEEE Engineering in Medicine and Biology - Proceedings*, 2006.

[16] N. Roussel, C. A. Morton, F. P. Finger, and B. Roysam, "A computational model for C. elegans locomotory behavior: Application to multiworm tracking," *IEEE Trans. Biomed. Eng.*, 2007.

[17] S. Faumont et al., "An Image-Free Opto-Mechanical system for creating virtual environments and imaging neuronal activity in freely moving caenorhabditis elegans," *PLoS One*, vol. 6, no. 9, 2011.

[18] J. H. Baek, P. Cosman, Z. Feng, J. Silver, and W. R. Schafer, "Using Machine Vision to Analyze and Classify Caenorhabditis elegans Behavioral Phenotypes Quantitatively," *Journal of Neuroscience Methods*, vol. 118, no. 1, pp. 9–21, 2002.

[19] W. R. Schafer, "Deciphering the Neural and Molecular Mechanisms of C. elegans Behavior," *Current Biology*, vol. 15, no. 17, pp. 723–729, 2005.

[20] S. Dong, X. Liu, Y. Lin, M. Kojima and T. Arai. "Automated Tracking System for Time Lapse Observation of C. elegans," in *Proc. of 2018 IEEE Int. Conf. on Mechatronics and Automation,* 2018*,* pp. 504-509.

[21] M. Maru, Y. Igarashi, S. Arai and K. Hashimoto. "Fluorescent microscope system to track a particular region of C. elegans," in *Proc. of IEEE/SICE Int. Symposium on System Integration: SI Int. 2010 - The 3rd Symposium on System Integration*, pp. 347-352, 2010.

[22] X.C. He and N.H.C. Yung. "Curvature Scale Space Corner Detector with Adaptive Threshold and Dynamic Region of Support," in *Proc. of the 17th Int. Conf. on Pattern Recognition,* pp. 791-794, 2004.

[23] L. Shao, H. Zhou. "Curve Fitting with Bezier Cubics," *Graph. Model. Image Process.,* vol. 58.3, pp. 223-232, 1996.

[24] A. Rosenfeld and E. Johnston, "Angle Detection on Digital Curves," *IEEE Trans. Comput*., vol. 22, no. 9, pp. 875-878, 1973.

[25] F. Pla, "Recognition of partial circular shapes from segmented contours," *Comput. Vis. Image Underst.*, vol. 63, no. 2, pp. 334-343, 1996.

[26] Redmon, Joseph and Farhadi, Ali, "YOLO9000: Better, Faster, Stronger", in *IEEE Conf. on Comput. Vision and Pattern Recognition 2017*, pp. 6517-6525, 2017.

[27] S. Takagi, and K. Ohara, and M. Kojima, and Y. Mae, "Improving the speed of 3D information presentation in a microhabitat", *IEEE Int. Conf. on Mechatronics and Automation 2013*, pp. 249-254, 2013.